



Fractal Elasticity

Final Year Project



Students' Names:

Dara Corr, Tian Yu Lim

National University of Ireland, Galway

Project Supervisor:

Dr. Giuseppe Zurlo



Abstract

Fractals are a fascinating, infinitely self-repeating pattern that seems to reappear again and again in nature. We ask ourselves, why does Nature seem to choose these kind of structures so often? Do they offer a mechanical advantage to other kind of designs in nature. This article aims to establish a connection between elasticity and optimal flow to the formation of fractal-like objects that occur in nature. We suspect there is some balancing between the two aspects that gave rise to favoring self-similar structures. We created a model which looks at the self-similar branching patterns that occur in living organisms such as in blood vessels or in lungs. We considered the flow of fluids through these branching paths as well as the stiffness of these designs and made a link between them. This model addresses some of the questions as to why fractals are important and so frequent in Nature.

Contents

1	Introduction	3
2	Definition of Fractals	3
2.1	Fractal dimension	4
2.2	Fractal trees and Horton Laws [1]	6
3	Mathematical Models	7
3.1	Optimal Channel Networks	7
3.2	Optimal Transport	8
3.3	Elasticity of Fractal Structures	11
3.4	Deriving Stiffness Matrices For Sierpinski Gasket (Triangle)	12
3.5	Deriving the Stiffness Matrix for a beam	15
3.6	Creating Stiffness Matrix for Branching tree fractal	20
4	Conclusions and Perspectives	24
5	Bibliography	25



1 Introduction

This project was conducted in order to analyse systems which possess a fractal or fractal-like structure and to see if it is possible to develop a theory of elasticity and mechanics around these these systems. We look at structures with fractal designs because these are very common in Nature and by investigating the elastic properties of these structures we hope to address why nature has a tendency to choose fractal paths and designs in the world around us. By designing a theory of Elasticity for fractals, we can simulate deformations of these bodies, analyse the stiffness of the structures and we can find the elastic energy in fractal like structures for example.

We also looked at the flow of media through these fractal structure to see if nature chooses these fractal designs to optimise flow as well as stiffness. By applying the understanding of the mechanics and elasticity of fractal structures to phenomena in nature, we can learn about the underlying mathematics and how the fractal design of these systems characterises the overall behaviour of the systems. We want to know what relationships fractal geometry have with mechanics and we want to develop a fractal theory of mechanics and elasticity to better learn why Fractals are found so commonly in Nature.

First we set out to understand fractals. In the first chapter of this report we define what fractals are and we talk about some famous fractals and how they are constructed. Then we start to look at Tree Fractals which are fractals that split into multiple branches at each iteration giving a tree-like pattern which is very commonly seen in nature.

We start to look at mathematical models for fractals. We focused on branching fractals' Optimal Transport and Stiffness. We look at existing models for branching fractals and we try to adapt them for our own model looking at Elasticity and Optimal flow of our branching tree model.

From our model we make conclusions on why Fractals occur on nature and what other information we can deduce from our model.

2 Definition of Fractals

Fractal geometry describes the irregular geometry of repeating geometric structures which cannot be described by classical geometries. A Fractal is a curve or geometrical figure, which has a never-ending, pattern which repeats itself to infinity. These kinds of geometries are characterised by their self-repeating nature. Magnifying a fractal image will result in an image with a similar geometrical pattern to the original image but with smaller dimensions. The most famous example of a Fractal is the Mandelbrot Fractal but they can be seen everywhere where there is self-repeating geometry such as the branching of tree branches and veins or the structure of clouds or the crystals of snowflakes.

This self-similarity property is seen in all Fractal structures. In Fractals in Nature, Fractals are only self-similar to a certain point unlike a theoretical fractal which repeat until infinity. Structures in Nature are limited by physical restrictions at smaller scales, for example fractals in plants are limited by the size of cells or atoms at smaller scales.

Here are two more common examples of fractals here are the Koch Snowflake and Sierpinski triangle pictured below.

The Koch Snowflake here is a Fractal model of a snowflake conceptualised by Helge Von Koch in 1904. It is constructed by taking a Equilateral Triangle and at each iteration of the fractal, divide each line on the triangle into 3 parts of equal length $\frac{L}{3}$. The middle part of each line L is removed and replaced with an equilateral triangle triangle of side length $\frac{L}{3}$ and remove the base of this triangle. Infinitely many iterations are applied to give us the famous Von Koch Snowflake.

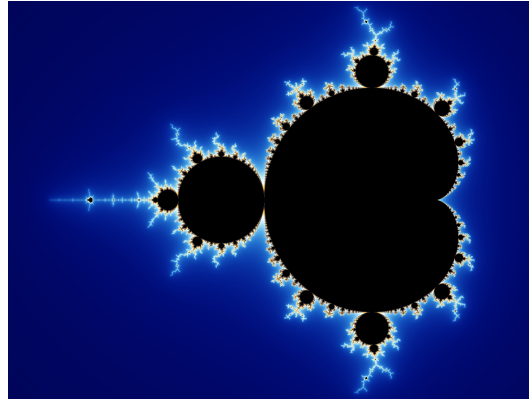


Figure 1: Mandelbrot Set

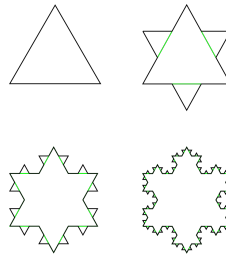


Figure 2: Koch Snowflake

The Von Koch Snowflake has some interesting properties, for example, the perimeter of the Von Koch Snowflake tends to ∞ whereas a simple computation shows that the Area of the Snowflake tends to $\frac{8}{5}$ the original area of the line.

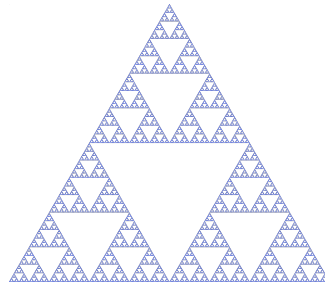


Figure 3: Sierpinski Triangle

Another Very interesting Fractal is the Sierpinski Gasket (Triangle). This Fractal begins with a Equilateral Triangle. And at each iteration, the Triangle is split into 4 smaller triangles and the inner portion is removed. The Perimeter of this Fractal tends to Infinity while the Area of the Gasket tends to zero which is in contrast to the Von Koch Snowflake mentioned previously.

2.1 Fractal dimension

Fractal Geometry cannot be easily described by traditional geometries. Since fractals repeat until infinity, it is not as straightforward to talk about things like length and Area of fractals and this gets more difficult



for more complicated examples of fractals. Fractals do not lie in the 3 topological dimensions we are used to (1-d, 2-d and 3-d space).

One useful property for analysing fractals is the concept of fractal dimension. Benoit Mandelbrot developed the concept of Fractal Dimension to try and explain the complexity of fractals and how Fractals lie somewhere within the topological dimensions. Mandelbrot famously computed the Fractal Dimension of Great Britain and found it to be $FD = 1.25$. The idea is to see how many self similar pieces that the original shape can contain after the size of that shape is shrunk by some magnification factor.

For example, if a line is shrunk down to half of its size, then the original line can contain 2 copies of the smaller line. ($2^1 = 2$)

A square plane can contain 4 copies of itself with magnification of 2. ($2^2 = 4$)

Similarly, a cube can break into 8 smaller pieces with magnification factor of 2. ($2^3 = 8$)

A pattern can be seen here as

$$S^D = N$$

We can then define fractal dimension D as

$$D = \frac{\log(N)}{\log(S)}$$

where N is the number of self-similar pieces and S is the scaling factor.

$$\text{fractal dimension} = \frac{\log(\text{self-similar pieces})}{\log(\text{scaling factor})}$$

Take a Von Koch Curve, its length increases by a factor of $4/3$ for each iteration. In a limiting sense, a Koch curve will have an infinite length and with zero area, which is not a useful notion. This is when fractal dimension comes in handy.

We know that scaling the Koch curve by $S = 3$ will also increase its "mass" by a factor of $N = 4$. Thus the fractal dimension is $(\log 4)/(\log 3) \approx 1.262$.

For Sierpinski Triangle, scaling it by $S = 2$ will contain $N = 3$ copies of itself, the fractal dimension is $(\log 3)/(\log 2) \approx 1.585$.

This formula is very effective for simple fractal structures but more complicated techniques are required to compute the Fractal Dimensions of more complex structures.

The **Minkowski–Bouligand dimension**, also known as **Minkowski dimension** or **box-counting dimension** is a different way of estimating the fractal dimension.

Imagine a fractal lying on a surface with evenly spaced grid and counting the total number of boxes that covers the set. It is easy to see that the number of boxes and the scaling factor will have a relation of

$$N = N_0 S^D$$

where N here represents the "mass" of fractal and N_0 is the initial number of boxes touched before scaling.

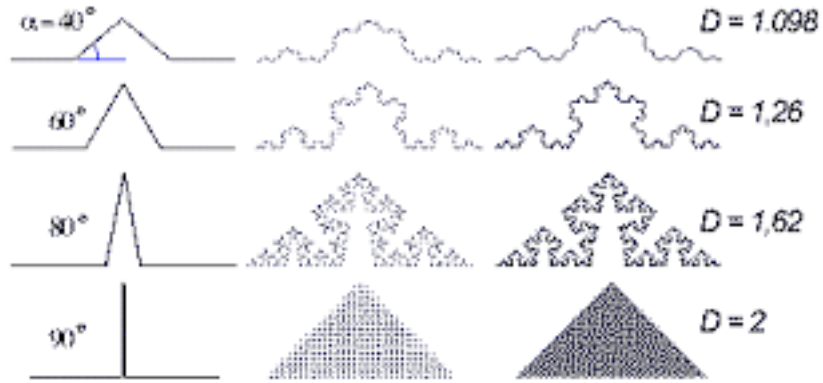


Figure 4: Fractal dimension of Koch curves with different angles

2.2 Fractal trees and Horton Laws [1]

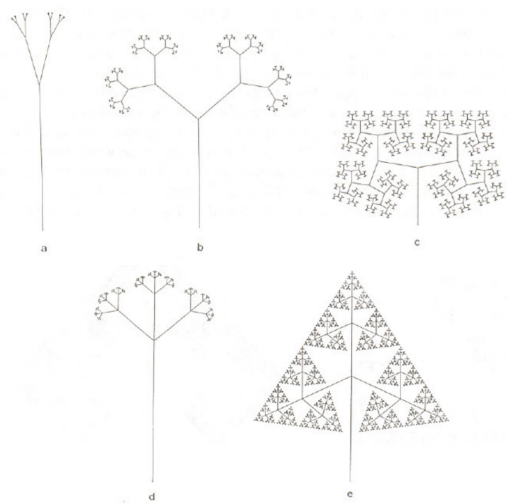


Fig. 1. Five different fractal trees. The corresponding N , r , and Θ values to generate them are (a) $N = 2$, $r = 1/3$, $\Theta = 30^\circ$, (b) $N = 2$, $r = 1/2$, $\Theta = 60^\circ$, (c) $N = 2$, $r = 2/3$, $\Theta = 80^\circ$, (d) $N = 3$, $r = 1/3$, $\Theta = 30^\circ$, (e) $N = 3$, $r = 1/2$, $\Theta = 120^\circ$.

Figure 5: Fractal Trees

Horton Law

There is a linear relationship between the logarithm of the number N_u of branches of order u vs. the order [1]

$$\log N = m(k - u)$$

then

$$m = \log N_u - \log N_{u+1}$$

and



$$10^m = \frac{N_u}{N_{u+1}} = r_B$$

where r_B is bifurcation ratio.

First line of equation can then be expressed as

$$N = r_B^{(k-u)}$$

3 Mathematical Models

3.1 Optimal Channel Networks

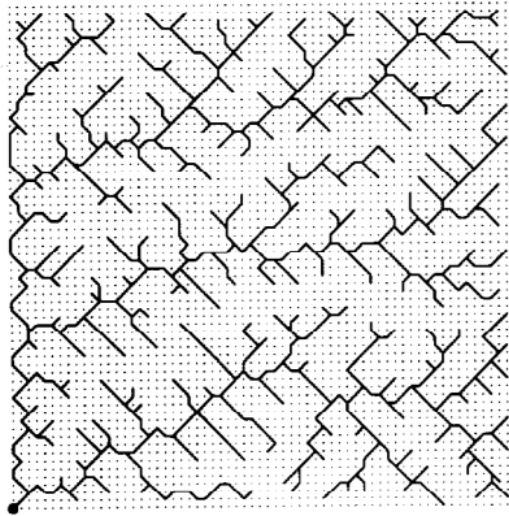


Figure 6: An example of generated OCN [2]

Two local principles postulate (1) minimum energy expenditure in any link of the network and (2) equal energy expenditure per unit area of channel anywhere in the network, yielding the rate P_i of energy expenditure at i -th link in the form [2]

$$P_i = \chi Q_i^{0.5} L_i$$

where Q_i is mean annual flow of i -th link and L_i is link length

(3) global principle of minimum energy expenditure such that

$$\sum_i P_i = \chi \sum_i Q_i^{0.5} L_i = \text{minimum}$$

This model suggests that fractals can occur under conditions such as minimizing the energy needed during its formation. We do not go into analyzing the details on this model due to the fact that it is more numerical from the start.



3.2 Optimal Transport

This section discusses the formation of fractal structure from the aspect of optimal flow.

Suppose there is a source (labelled D) wants to deliver some substance (ie. fluids) to two sinks A and B, with C as the point where the flow splits into two. Depending on the pipe diameter ratio after splitting, there is a certain point where the shape of the whole structure starts to change.

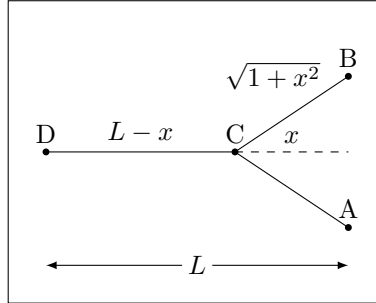


Figure 7: Flow from one source to two sinks

This model only considers 2-dimensional branching and does not include gravitational potential (Imagine the pipes are laying on a flat surface).

Length of the model from left to right is L , sink A and sink B are placed symmetrically at the right end 1 unit distance away from the center line. Point C is only free to move horizontally and is x distance away from the right end. The reason we keep the distance between the two sinks fixed is because it is only necessary to scale the length L accordingly to change the geometry of the system.

We now define

$$\Delta p = cQ, \quad c = \frac{l}{d^4}, \quad p_A = p_B = p_0, \quad d_1 = \beta d_0$$

where pressure drop across a pipe Δp is proportional to the flow rate Q it contains, its length l and is inversely proportional to the pipe diameter d^4 . Pressure at sinks A and B are the same for some constant p_0 . Diameter of pipe before and after branching is d_0 and d_1 respectively. The goal is to obtain minimum pressure based on the location of C .

We'll start by considering pressure at C

$$p_C = p_0 + \Delta p_{CA} = p_0 + \Delta p_{CB}$$

So

$$\Delta p_{CA} = \Delta p_{CB}$$

$$Q_{CA} = Q_{CB}$$

Since $Q_{DC} = Q_{CA} + Q_{CB}$, thus $Q_{CB} = \frac{1}{2}Q_{DC}$

Now pressure at source is

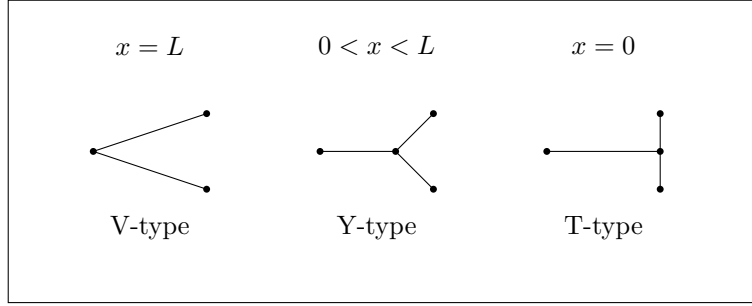


Figure 8: Different types of branching

$$\begin{aligned} p_D &= p_0 + \Delta p_{CB} + \Delta p_{DC} \\ &= p_0 + \frac{\sqrt{1+x^2}}{(\beta d_0)^4} \cdot \frac{1}{2} Q_{DC} + \frac{L-x}{d_0^4} Q_{DC} \end{aligned}$$

By setting the initial flow rate Q_{DC} constant, we can define a function that contains only variables related to the shape of the whole structure. That way minimizing the function also minimizes pressure required from the source.

$$f(x) := \frac{\sqrt{1+x^2}}{2(\beta d_0)^4} + \frac{L-x}{d_0^4}$$

and

$$f'(x) = \frac{1}{2(\beta d_0)^4} \frac{x}{\sqrt{1+x^2}} - \frac{1}{d_0^4}$$

To minimize the function take $f'(x) = 0$, then

$$x_{min} = \frac{2\beta^4}{\sqrt{1-4\beta^8}}$$

Note that the minimum point when pressure is lowest does not depend on length of the structure, it is always x_{min} unit distance away from the mid-point of the two sinks.

But when β is close to 1, the minimum point is larger than $x = L$ so that the pressure is lowest when $x = L$, and we want to find what diameter ratio can give non-trivial shapes. Y-type is said to be trivial and is not preferred because it branches off right at the start. This cannot form a fractal-like structure as it is always optimal to branch off straight from the source even there are more sinks presented in the system.

To find the maximum ratio in order to get Y-type structure, set $f'(L) = 0$,

$$\frac{1}{2(\beta d_0)^4} \frac{L}{\sqrt{1+L^2}} - \frac{1}{d_0^4} = 0$$

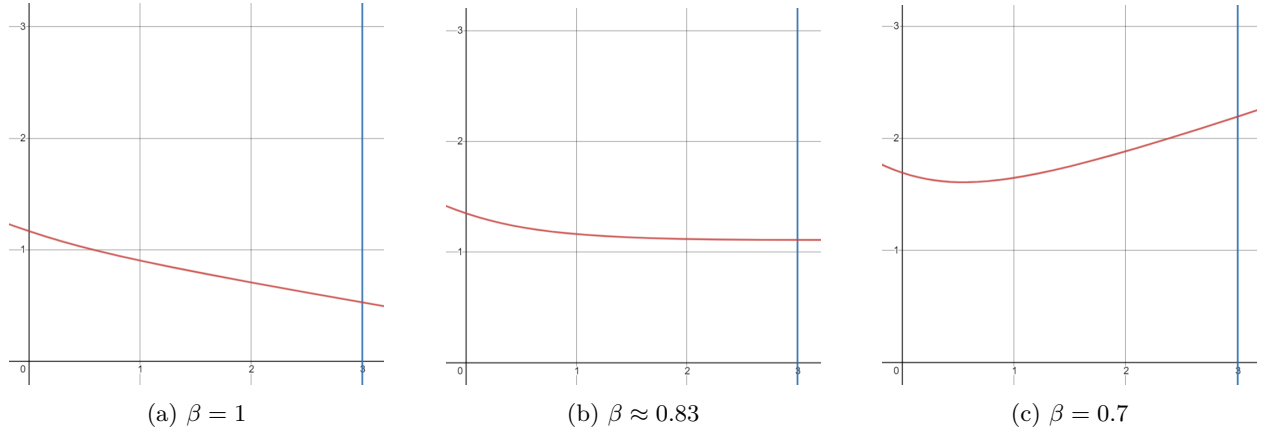


Figure 9: Function f depending on different values of β with $L = 3$

$$\beta_{max} = \left(\frac{L}{2\sqrt{1+L^2}} \right)^{\frac{1}{4}}$$

What about $x = 0$? It turns out that

$$f'(0) = -\frac{1}{d_0^4} < 0$$

which is always negative. This means that the pressure is always decreasing when the branching point is moving away from the source. So the result is that T-type structure is not preferred in every type of scenario.

Murray's Law provides a relation between branching thicknesses by minimizing the power of transport as well as the power to maintain the transport medium, by the following:

$$r^3 = r_1^3 + r_2^3 + \dots + r_n^3$$

where r is the radius of parent branch and r_1, \dots, r_n are the radii of child branches.

For our case we only have two splitting branches, so $r_1 = r_2$,

$$r^3 = 2r_1^3$$

The diameter ratio arrived from Murray's Law is

$$\beta = \frac{r_1}{r} = \left(\frac{1}{2} \right)^{\frac{1}{3}} \approx 0.79$$

we expect this will be the diameter ratio that gives the lowest cost of transport.

Minimum point when the diameter ratio is at this value

$$x_{opt} \approx 1.3$$



3.3 Elasticity of Fractal Structures

For our analysis of elasticity in fractal structures we decided to use the Finite Element Method — (Direct Stiffness Method) to calculate the stiffness of structures

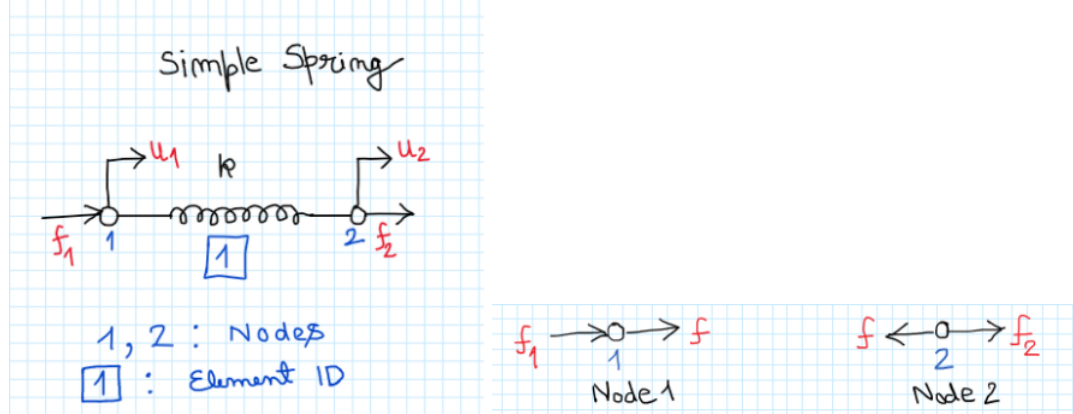


Figure 10: Simple spring stiffness matrix derivation [3]

$$\begin{aligned}
 f_1 + f &= 0 \\
 f_1 + k(u_2 - u_1) &= 0 \\
 f_1 &= k(u_1 - u_2)
 \end{aligned}
 \qquad
 \begin{aligned}
 f_2 - f &= 0 \\
 f_2 - k(u_2 - u_1) &= 0 \\
 f_2 &= -k(u_1 - u_2)
 \end{aligned}$$

Combining two equations above in matrix form:

$$\begin{Bmatrix} f_1 \\ f_2 \end{Bmatrix} = \begin{bmatrix} k & -k \\ -k & k \end{bmatrix} \begin{Bmatrix} u_1 \\ u_2 \end{Bmatrix}$$

In general,

$$\mathbf{F} = \mathbf{K}\mathbf{U}$$

where \mathbf{K} is an $(n \times n)$ stiffness matrix for n degree of freedoms.

Elastic energy stored:

$$\begin{aligned}
 W &= \frac{1}{2}(k_1 u_1^2 + k_2 u_2^2 + \cdots + k_n u_n^2) \\
 &= \frac{1}{2}(f_1 u_1 + f_2 u_2 + \cdots + f_n u_n) \\
 &= \frac{1}{2} \mathbf{F}^T \mathbf{U} \\
 &= \frac{1}{2} (\mathbf{K}\mathbf{U})^T \mathbf{U} \\
 &= \frac{1}{2} \mathbf{U}^T \mathbf{K}^T \mathbf{U} \\
 &= \frac{1}{2} \mathbf{U}^T \mathbf{K} \mathbf{U}
 \end{aligned}$$



3.4 Deriving Stiffness Matrices For Sierpinski Gasket (Triangle)

The Stiffness matrix of a system with a fractal structure can be found by considering boundary conditions and degrees of freedom of the system. The stiffness matrix is then dependent on the degrees of freedom the system has. For a system of N degrees of freedom we will have a $N \times N$ stiffness matrix.

The stiffness of the reduced fractal system when zoomed in is related to the stiffness of the original system before reduction. They are related by a proportionality constant. [4] [5]

$$K = \alpha k$$

For example, the

Where α is normally ≤ 1

To compute the stiffness matrix of an object we must first consider the degrees of freedom of the object. Here we will consider The Sierpinski Gasket (triangle) which begins with an equilateral triangle with sides of length L . An inner triangle of length $\frac{L}{2}$ is removed at the first step leaving 3 outer triangles with a vacant triangle in the centre. For the next step of generating the Gasket, the previous step is applied to the remaining smaller 3 triangles. These steps can be applied an infinite number of times, giving us the iconic Sierpinski Gasket Fractal.

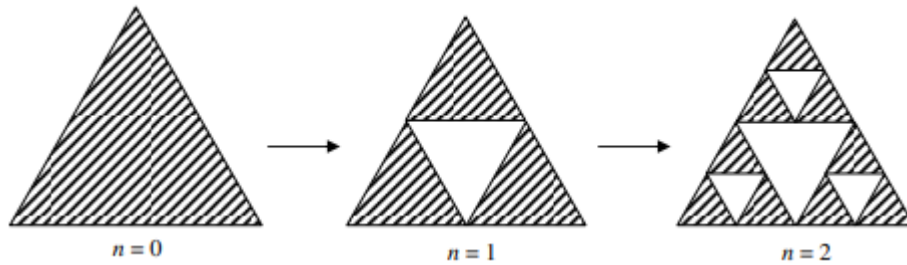


Figure 11: Generation of Sierpinski Gasket courtesy of Epstein et al. [5]

We impose 3 restrictions when computing the stiffness matrix for the Sierpinski Triangle.

1) Restrictions due to Elasticity: Stiffness matrix is positive definite due to the conservation of energy and thus is a symmetric matrix. Because of this there are 21 unique entries we are concerned with in this matrix.

Before we compute the stiffness matrix for the Sierpinski Gasket, we start by finding the stiffness matrix for An Equilateral Triangle using figure 12(b) (the local configuration for DOFs of equilateral triangle).

2) Apply restrictions due to Geometric symmetries. We find the following relations hold:

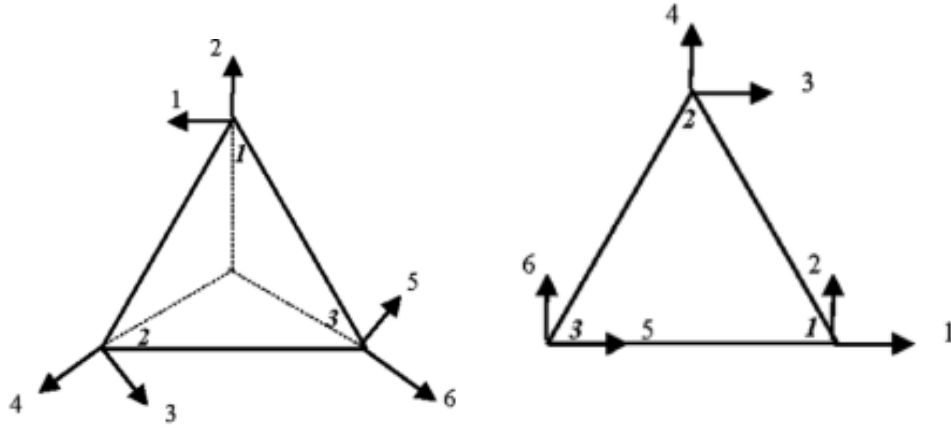


Figure 12: Degrees of Freedom for Stiffness matrix of Equilateral Triangle (local and global configuration) courtesy of Epstein et al. [4]

$$\begin{aligned}
 K_{11} &= K_{33} = K_{55} = A \\
 K_{22} &= K_{44} = K_{66} = B \\
 K_{12} &= K_{34} = K_{56} = 0 \\
 K_{13} &= K_{35} = K_{51} = C \\
 K_{14} &= K_{36} = K_{52} = D \\
 K_{23} &= K_{45} = K_{61} = E \\
 K_{24} &= K_{46} = K_{62} = F
 \end{aligned}$$

3) Apply Restrictions due to equilibrium: Net Forces in Horizontal and Vertical directions about the centroid of the triangle should be zero. Each Column j in the stiffness matrix represents a set of forces due to unit displacement of a degree of freedom. Imposing Equilibrium leads to the following conditions:

$$\begin{aligned}
 K_{1j} - 0.5(K_{3j} + K_{5j}) + \sqrt{3}/2(K_{4j} - K_{6j}) &= 0 \\
 K_{2j} - 0.5(K_{4j} + K_{6j}) - \sqrt{3}/2(K_{3j} - K_{5j}) &= 0 \\
 K_{1j} + K_{3j} + K_{5j} &= 0
 \end{aligned} \tag{1}$$

The Stiffness Matrix for the Equilateral Triangle is then:

$$\mathbf{K}_1 = \begin{bmatrix} A & 0 & -\frac{A}{2} & -\frac{\sqrt{3}A}{2} & -\frac{A}{2} & -\frac{\sqrt{3}A}{2} \\ & B & \frac{\sqrt{3}A}{2} & B - \frac{3A}{2} & -\frac{\sqrt{3}A}{2} & B - \frac{3A}{2} \\ & & A & 0 & -\frac{A}{2} & -\frac{\sqrt{3}A}{2} \\ & & & B & \frac{\sqrt{3}A}{2} & B - \frac{3A}{2} \\ & & & & A & 0 \\ & & & & & B \end{bmatrix}$$

Symmetric

To assemble three equilateral triangles together we need to use the global configuration for the degrees of freedom in figure 12(a). A rotation of the degrees of Freedom gives the following matrix:



$$\mathbf{K} = \begin{bmatrix} \frac{A+3B}{4} & \frac{\sqrt{3}(A-B)}{4} & -\frac{A}{2} & -\frac{\sqrt{3}(B-2A)}{2} & \frac{A-3B}{4} & \frac{\sqrt{3}(3A-B)}{4} \\ & \frac{3A+B}{4} & \frac{\sqrt{3}A}{2} & -\frac{B}{2} & \frac{\sqrt{3}(B-3A)}{4} & \frac{B-3A}{4} \\ & & A & 0 & -\frac{A}{2} & -\frac{\sqrt{3}A}{2} \\ & & & B & \frac{\sqrt{3}(2A-B)}{2} & -\frac{B}{2} \\ & \text{Symmetric} & & & \frac{A+3B}{4} & \frac{\sqrt{3}(B-A)}{4} \\ & & & & & \frac{3A+B}{4} \end{bmatrix}$$

Also using the fact that α is found to be $1/2$ and the ratio B/A is found to be equal to 3, then the final stiffness matrix of a Sierpinski gasket has the form:

$$\mathbf{K} = \begin{bmatrix} \frac{5}{2} & -\frac{\sqrt{3}}{2} & -\frac{1}{2} & -\frac{\sqrt{3}}{2} & -2 & 0 \\ & \frac{3}{2} & \frac{\sqrt{3}}{2} & -\frac{3}{2} & 0 & 0 \\ & & 1 & 0 & -\frac{1}{2} & -\frac{\sqrt{3}}{2} \\ & & & 3 & -\frac{\sqrt{3}}{2} & -\frac{3}{2} \\ & \text{Symmetric} & & & \frac{5}{2} & \frac{\sqrt{3}}{2} \\ & & & & & \frac{3}{2} \end{bmatrix} A$$

For a given constant A we can find out the stiffness of the Sierpinski Triangle or any of the smaller reduced triangles that lie within it. A smaller triangle within the Sierpinski triangle has $2 \times$ greater stiffness than the parent triangle it lies within because the proportionality constant for the Sierpinski Triangle is $1/2$.

We apply a similar technique to developing a stiffness matrix for a branched fractal structure in section 3.6



3.5 Deriving the Stiffness Matrix for a beam

Computing Stiffness Matrix of a beam (frame element):

A stiffness matrix K of a structure is a $N \times N$ matrix for a system with N degrees of freedom with each entry k_{ij} representing the reaction of a support corresponding to a degree of freedom i due to a unit displacement of the support corresponding to the degree of freedom number j

Before we try to derive the stiffness matrices for our fractal model, first we will derive the stiffness matrix for a simple beam of length L with 6 degrees of freedom, 3 at each node (2 translational DOFs and one Rotational DOF) using the Finite Element Method (FEM).

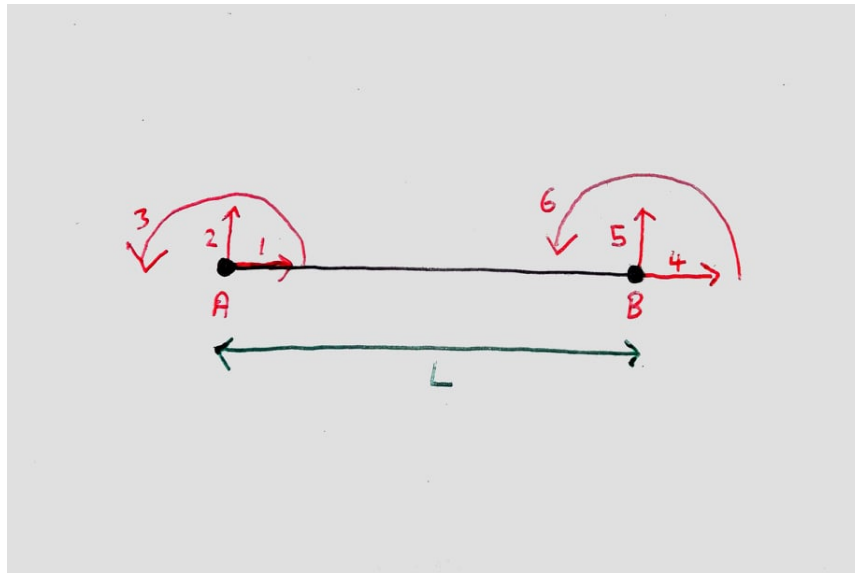


Figure 13: Beam with 6 degrees of freedom

First we look at a column with 1 DOF. The force-displacement relationship is described as $F = k\delta$. Here k is the stiffness of the system and it is given by $\frac{EA}{L}$ in this case. E is the modulus of elasticity of the material, A is the cross sectional area of the column and L is the length of the column. EA is called the Axial stiffness of the beam.

Now we look at a beam with 2 degrees of freedom. We make the assumption that $\delta_1 > \delta_2$ so that

$$F_1 = \frac{AE}{L}(\delta_1 - \delta_2) = \frac{AE}{L}\delta_1 - \frac{AE}{L}\delta_2$$

and then by assuming that there is equilibrium in the x direction:

$$F_2 = -F_1$$

$$F_2 = -\frac{AE}{L}(\delta_1 - \delta_2) = \frac{AE}{L}\delta_2 - \frac{AE}{L}\delta_1$$

We can write this system in matrix form:

$$F = K\delta$$

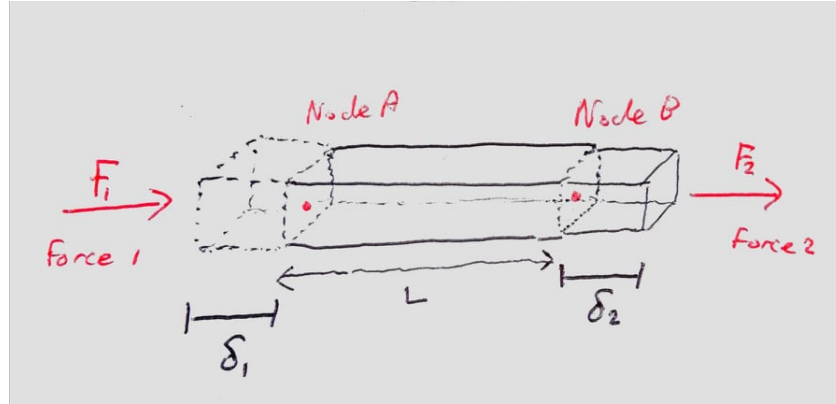


Figure 14: Beam with 2 Degrees of Freedom

$$\begin{bmatrix} F1 \\ F2 \end{bmatrix} = \begin{bmatrix} \frac{AE}{L} & -\frac{AE}{L} \\ -\frac{AE}{L} & \frac{AE}{L} \end{bmatrix} \begin{bmatrix} \delta_1 \\ \delta_2 \end{bmatrix}$$

Next we look at a beam with 4 Degrees of Freedom, 2 DOFs at each end. Each end has a vertical translational degree of freedom as well as a rotational degree of freedom which correspond to a Force in the y-direction on each node causing the translational movement and a Moment acting on each node causing the rotational movement.



Figure 15: Beam with 4 Degrees of Freedom

We will derive the associated stiffness matrix for this system now which will be in the form of:

$$\begin{Bmatrix} F_1 \\ M_1 \\ F_2 \\ M_2 \end{Bmatrix} = \begin{bmatrix} k_{11} & k_{12} & k_{13} & k_{14} \\ k_{21} & k_{22} & k_{23} & k_{24} \\ k_{31} & k_{32} & k_{33} & k_{34} \\ k_{41} & k_{42} & k_{43} & k_{44} \end{bmatrix} \begin{Bmatrix} v_1 \\ \theta_1 \\ v_2 \\ \theta_2 \end{Bmatrix}$$



First we assume a displacement function of

$$V(x) = a_1x^3 + a_2x^2 + a_3x + a_4$$

This function provides 4 degrees of freedom so it is an appropriate choice. We note that $\frac{dv}{dx} = \theta$ is rotation in Nm/rad and v is vertical displacement in m.

We apply boundary conditions on the beam:

- take a_4 as the displacement at $x = 0$: $V(0) = v_1 = a_4$
- slope at node 1 = derivative of displacement at node 1: $\frac{dV(0)}{dx} = \theta_1 = a_3$
- define displacement at $x = L$ as:

$$V(L) = v_2 = a_1L^3 + a_2L^2 + \theta_1L + v_1 \quad (2)$$

- define rotation at $x = L$ as:

$$\frac{dV(L)}{dx} = \theta_2 = 3a_1L^2 + 2a_2L + \theta_1 \quad (3)$$

Solving equations 1 and 2, we found:

$$a_1 = \frac{2}{L^3}(v_1 - v_2) + \frac{1}{L^2}(\theta_1 + \theta_2)$$

$$a_2 = \frac{-3}{L^2}(v_1 - v_2) - \frac{1}{L}(2\theta_1 + \theta_2)$$

we sub these into our equation for V(x)

$$V(x) = \left[\frac{2}{L^3}(v_1 - v_2) + \frac{1}{L^2}(\theta_1 + \theta_2) \right] x^3 + \left[-\frac{3}{L^2}(v_1 - v_2) - \frac{1}{L}(2\theta_1 + \theta_2) \right] x^2 + a_3x + a_4$$

Before we start using our new displacement function to derive the stiffness matrix for the beam we must note sign conventions, since Beam Theory uses different sign conventions to what we are using here with the stiffness method.

Now we can apply some equations from beam theory in order to obtain the stiffness matrix for our beam:

From beam theory we know that a Moment for a node at a point x on the beam is:

$$M(x) = \frac{d^2V(x)}{dx^2}EI \quad (4)$$

and force at a point x is:

$$F(x) = \frac{d^3V(x)}{dx^3}EI \quad (5)$$

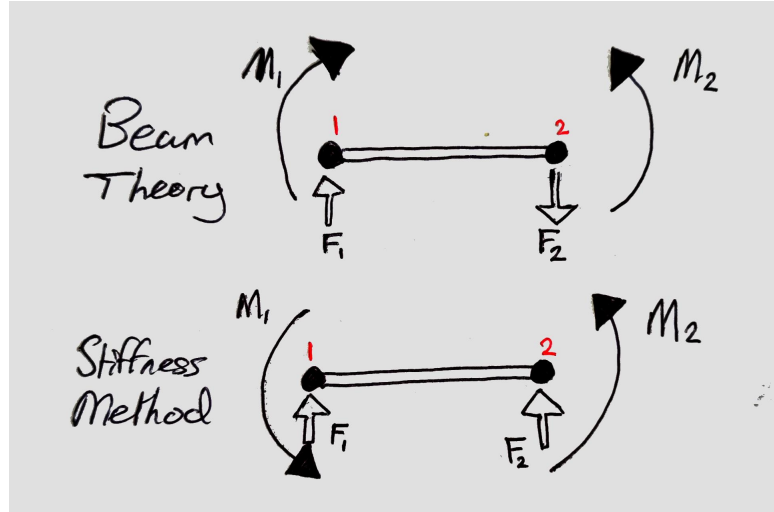


Figure 16: Sign Conventions for Beam Theory and Stiffness Method

Using Equations 3 and 4 and taking sign conventions into account we get a system of equations describing the relationship between Forces, Momenents and their corresponding Displacements and rotations on the beam:

$$\begin{aligned}
 F_1 &= +F_{beam} = EI \frac{d^3 V(0)}{dx^3} = \frac{EI}{L^3} [12v_1 6L\theta_1 - 12v_2 + 6L\theta_2] \\
 M_1 &= -M_{beam}(0) = -EI \frac{d^2 V(0)}{dx^2} = \frac{EI}{L^3} [6Lv_1 + 4L^2\theta_1 - 6Lv_2 + 2L^2\theta_2] \\
 F_2 &= -F_{beam} = -EI \frac{d^3 V(L)}{dx^3} = \frac{EI}{L^3} [-12v_1 - 6L\theta_1 + 12v_2 - 6L\theta_2] \\
 M_2 &= +M_{beam}(L) = +EI \frac{d^2 V(L)}{dx^2} = \frac{EI}{L^3} [6Lv_1 + 2L^2\theta_1 - 6Lv_2 + 4L^2\theta_2]
 \end{aligned}$$

This can be put in Matrix form $F = Kd$ which gives us our Stiffness Matrix K for the simple beam.

$$\begin{Bmatrix} F_{1y} \\ M_1 \\ F_{2y} \\ M_2 \end{Bmatrix} = \frac{EI}{L^3} \begin{bmatrix} 12 & 6L & -12 & 6L \\ 6L & 4L^2 & -6L & 2L^2 \\ -12 & -6L & 12 & -6L \\ 6L & 2L^2 & -6L & 4L^2 \end{bmatrix} \begin{Bmatrix} v_1 \\ \theta_1 \\ v_2 \\ \theta_3 \end{Bmatrix}$$

We can combine the Axial Stiffness Matrix for the first Beam (Truss) with 2 DOFS (2×2 matrix) with the 4×4 stiffness matrix for the beam we just derived to find the stiffness matrix (6×6 matrix) of a Frame element as pictured here:

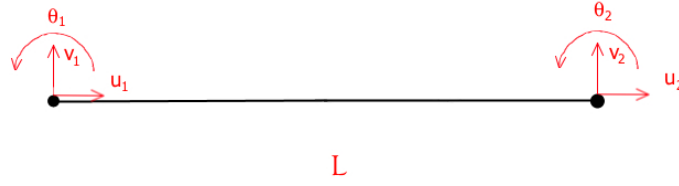


Figure 17: Frame element (beam) with 6 Degrees of Freedom

The Stiffness Matrix equation for the 6 DOF beam is:

$$\begin{Bmatrix} F_{1x} \\ F_{1y} \\ M_1 \\ F_{2x} \\ F_{2y} \\ M_2 \end{Bmatrix} = \frac{E}{L} \begin{bmatrix} A & 0 & 0 & -A & 0 & 0 \\ 0 & \frac{12I}{L^2} & \frac{6I}{L} & -\frac{12I}{L^2} & 0 & \frac{6I}{L} \\ 0 & \frac{6I}{L} & 4I & 0 & -\frac{6I}{L} & 2I \\ -A & 0 & 0 & A & 0 & 0 \\ 0 & -\frac{12I}{L^2} & -\frac{6I}{L} & 0 & \frac{12I}{L^2} & -\frac{6I}{L} \\ 0 & \frac{6I}{L} & 2I & 0 & -\frac{6I}{L} & 4I \end{bmatrix} \begin{Bmatrix} u_1 \\ v_1 \\ \theta_1 \\ u_2 \\ v_2 \\ \theta_2 \end{Bmatrix}$$

so the stiffness matrix is then given by :

$$K_{beam} = \frac{E}{L} \begin{bmatrix} A & 0 & 0 & -A & 0 & 0 \\ 0 & \frac{12I}{L^2} & \frac{6I}{L} & -\frac{12I}{L^2} & 0 & \frac{6I}{L} \\ 0 & \frac{6I}{L} & 4I & 0 & -\frac{6I}{L} & 2I \\ -A & 0 & 0 & A & 0 & 0 \\ 0 & -\frac{12I}{L^2} & -\frac{6I}{L} & 0 & \frac{12I}{L^2} & -\frac{6I}{L} \\ 0 & \frac{6I}{L} & 2I & 0 & -\frac{6I}{L} & 4I \end{bmatrix}$$

We can use this Matrix equation to compute the vertical Force needed for a unit vertical displacement of the end of the bar while keeping the other end of the bar fixed (set $v_2 = 1$).

$$F_{2y} = \frac{12EI}{L^3}$$



Figure 18: beam with unit displacement $v_2 = 1$ due to Force $F_{2y} = \frac{12EI}{L^3}$



3.6 Creating Stiffness Matrix for Branching tree fractal

Now we combine what we learned about Fractals and the Finite Element Method of determining stiffnesses to compute the Stiffness Matrix for a branching tree Fractal. We decided to model this kind of design because it is very common in nature, such designs are commonly found in leaves, trees, lungs,

Our Model is constructed by taking a beam of Length L , dividing it into two beams of Length $\frac{L}{2}$. Now there are three nodes, 1,2 and 3, with node 2 shared by both beam segments. The second segment of the beam is removed and replaced with two branches (beam segments) of Length $L/2$ both starting from node 2 and rotated by an angle $\pm\theta$

The first 4 incidences of this fractal are pictured below (we took θ to be equal to 45°)

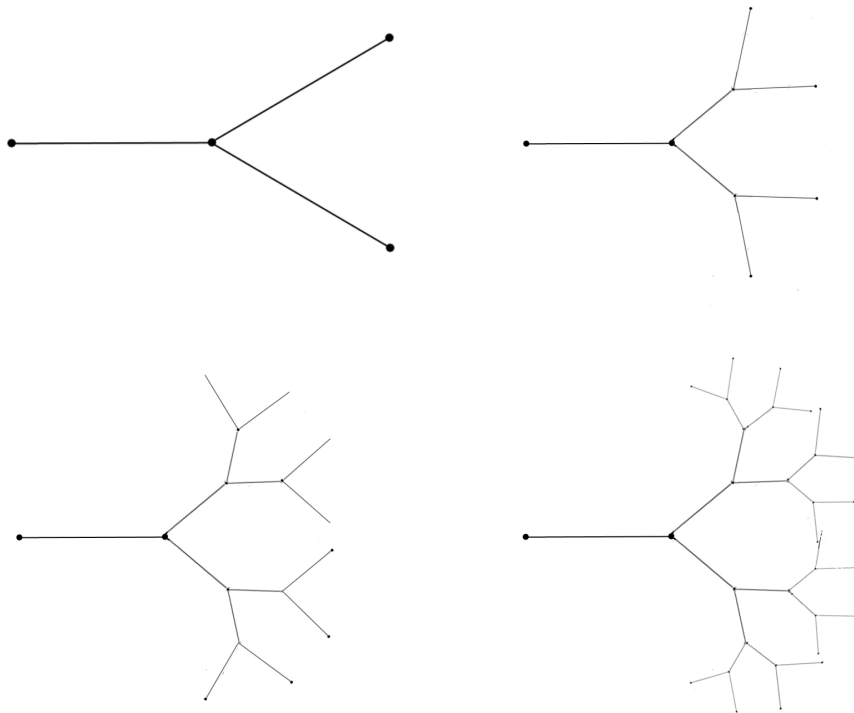


Figure 19: 1st 4 iterations of our branching tree Fractal model

We will mostly be concerned with the first iteration in our calculations. This branch contains three elements. We consider each element as a beam with 3 Degrees of Freedom at each node like we considered with the Beam (frame) element we derived previously. This system is made up of three elements with a total of 12 Degrees of Freedom in total so the stiffness matrix in this case will be a 12×12 matrix.

We will be working on determining the stiffness of this form of the branch. We label the degrees of freedom of each node i ($i = 1,2,3,4$) u_i, v_i and θ_i corresponding to the horizontal, vertical and rotational movements of each of the nodes. We define Element 1 is along the line segment between node 1 and node 2, element 2 is the segment comprised of nodes 2 and 3, and element 3 is the segment composed of node 2.

Element 1 has the same stiffness matrix as the Stiffness matrix we derived for the beam Previously. Elements 2 and 3 use the beam stiffness matrix as seen before but with a rotation applied to them. We will call the stiffness matrices for elements 1,2 and 3 $\mathbf{K}_1, \mathbf{K}_2$ and \mathbf{K}_3 respectively.

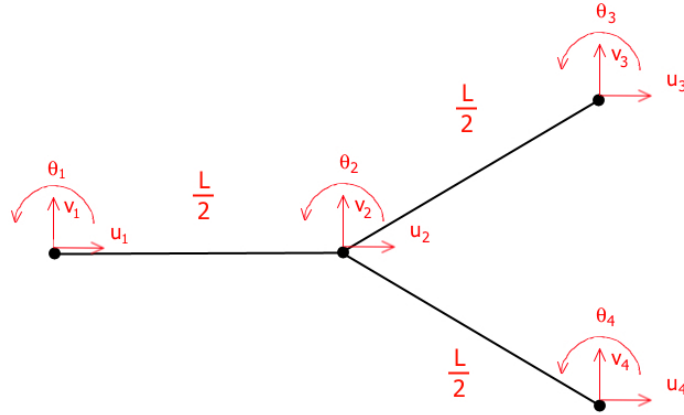


Figure 20: Branching fractal beam with 12 Degrees of Freedom

Our Equation involving Forces, stiffness and displacements is then of the form:

$$[F] = [\mathbf{K}_1][d_1] + [\mathbf{K}_2][d_2] + [\mathbf{K}_3][d_3] = [\mathbf{K}][d]$$

we apply rotation to the original stiffness matrix in local coordinates in order to obtain the rotated beam stiffness matrix for the global system.

$$\mathbf{K}_2 = R_+^T K R_+$$

$$\mathbf{K}_3 = R_-^T K R_-$$

where R is a rotation matrix in $\pm\theta$ and R^T is its transpose

$$R = \begin{bmatrix} \cos(\theta) & \sin(\theta) & 0 & 0 & 0 & 0 \\ -\sin(\theta) & \cos(\theta) & 0 & 0 & 0 & 0 \\ 0 & 0 & 1 & 0 & 0 & 0 \\ 0 & 0 & 0 & \cos(\theta) & \sin(\theta) & 0 \\ 0 & 0 & 0 & -\sin(\theta) & \cos(\theta) & 0 \\ 0 & 0 & 0 & 0 & 0 & 1 \end{bmatrix}$$

We find that for $\theta = \pm 45^\circ$

$$R_\pm^T K R_\pm = \frac{E}{L} \begin{bmatrix} \frac{1}{2}(A + \frac{12I}{L^2}) & \pm \frac{1}{2}(A - \frac{12I}{L^2}) & \mp \frac{6}{\sqrt{2}} \frac{I}{L} & -\frac{1}{2}(A + \frac{12I}{L^2}) & \mp \frac{1}{2}(A - \frac{12I}{L^2}) & \mp \frac{6}{\sqrt{2}} \frac{I}{L} \\ \pm \frac{1}{2}(A - \frac{12I}{L^2}) & \frac{1}{2}(A + \frac{12I}{L^2}) & \frac{6}{\sqrt{2}} \frac{I}{L} & \mp \frac{1}{2}(A - \frac{12I}{L^2}) & -\frac{1}{2}(A + \frac{12I}{L^2}) & \frac{6}{\sqrt{2}} \frac{I}{L} \\ \mp \frac{6}{\sqrt{2}} \frac{I}{L} & \frac{6}{\sqrt{2}} \frac{I}{L} & 4I & \pm \frac{6}{\sqrt{2}} \frac{I}{L} & -\frac{6}{\sqrt{2}} \frac{I}{L} & 2I \\ \frac{1}{2}(-A + \frac{12I}{L^2}) & \mp \frac{1}{2}(A - \frac{12I}{L^2}) & \pm \frac{6}{\sqrt{2}} \frac{I}{L} & \frac{1}{2}(A + \frac{12I}{L^2}) & \pm \frac{1}{2}(A - \frac{12I}{L^2}) & \pm \frac{6}{\sqrt{2}} \frac{I}{L} \\ \mp \frac{1}{2}(A - \frac{12I}{L^2}) & -\frac{1}{2}(A + \frac{12I}{L^2}) & -\frac{6}{\sqrt{2}} \frac{I}{L} & \pm \frac{1}{2}(A - \frac{12I}{L^2}) & \frac{1}{2}(A + \frac{12I}{L^2}) & -\frac{6}{\sqrt{2}} \frac{I}{L} \\ \mp \frac{6}{\sqrt{2}} \frac{I}{L} & \frac{6}{\sqrt{2}} \frac{I}{L} & 2I & \pm \frac{6}{\sqrt{2}} \frac{I}{L} & -\frac{6}{\sqrt{2}} \frac{I}{L} & 4I \end{bmatrix}$$



taking element 2 rotated by $\theta = +45^\circ$ and element 3 reotated by $\theta = +45^\circ$, then:

$$F_1 = \begin{Bmatrix} F_{1x} \\ F_{1y} \\ M_1 \\ F_{2x} \\ F_{2y} \\ M_2 \end{Bmatrix} = \mathbf{K}_1[d] = \mathbf{K}_1 \begin{Bmatrix} u_1 \\ v_1 \\ \theta_1 \\ u_2 \\ v_2 \\ \theta_2 \end{Bmatrix}$$

$$F_2 = \begin{Bmatrix} F_{2x} \\ F_{2y} \\ M_2 \\ F_{3x} \\ F_{3y} \\ M_3 \end{Bmatrix} = \mathbf{K}_2 \begin{Bmatrix} u_2 \\ v_2 \\ \theta_2 \\ u_3 \\ v_3 \\ \theta_3 \end{Bmatrix}$$

$$F_3 = \begin{Bmatrix} F_{2x} \\ F_{2y} \\ M_2 \\ F_{4x} \\ F_{4y} \\ M_4 \end{Bmatrix} = \mathbf{K}_3 \begin{Bmatrix} u_2 \\ v_2 \\ \theta_2 \\ u_4 \\ v_4 \\ \theta_4 \end{Bmatrix}$$

Note also that the force applied to the same node in different elements is the same for example $F_{2x}^{(1)} + F_{2x}^{(2)} + F_{2x}^{(3)} = F_{2x}$ where $F_{2x}^{(i)}$ denotes the horizontal force on node 2 for element i

Then our Stiffness Equation is as follows:

$$[F] = [K][d]$$

Where $[K]$ is a 12×12 vector with the 12 Forces/Moments of the systems in order and d is an ordered 12×1 vector containing the 12 DOFs of the system. K here is a 12×12 stiffness Matrix.

We can look at the forces on the beam when a shear force is applied to the two Branches of beam as follows.

We consider only vertical displacements v_2 , v_3 and v_4 and vertical forces F_5 , F_8 and F_{11} acting on nodes 2, 3 and 4.

$$F_5 = F_{2y} = E \left[\left(\frac{A}{L} + \frac{12I}{L} + \frac{12I}{L^3} \right) v_2 - \frac{1}{2} \left(\frac{A}{L} + \frac{12I}{L^3} \right) (v_3 + v_4) \right] = 0 \quad (6)$$

$$F_8 = F_{3y} = \frac{E}{2} \left[\left(\frac{A}{L} + \frac{12I}{L^3} \right) (v_3 - v_2) \right] \quad (7)$$

$$F_{11} = F_{4y} = \frac{E}{2} \left[\left(\frac{A}{L} + \frac{12I}{L^3} \right) (v_4 - v_2) \right] \quad (8)$$

note $F_5 = 0$ since no external force applied also note $F_8 = F_{11} = \frac{F}{2}$

solving for $F_5 = 0$ and $v_3 = v_4$ we find from equation 6:

$$\left(\frac{A}{L} + \frac{12I}{L} + \frac{12I}{L^3} \right) v_2 = \frac{1}{2} \left(\frac{A}{L} + \frac{12I}{L^3} \right) (v_3 + v_4)$$

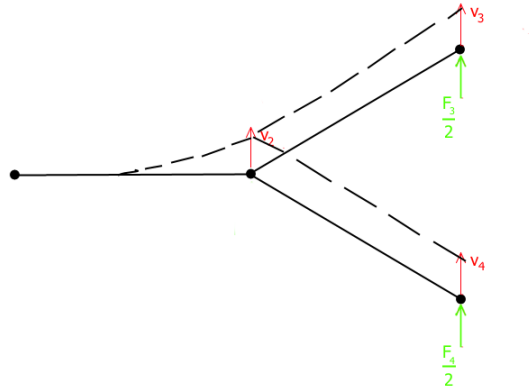


Figure 21: Applying a Force $F/2$ to both ends of the Branch

$$\left(\frac{A}{L} + \frac{12I}{L} + \frac{12I}{L^3}\right)v_2 = \left(\frac{A}{L} + \frac{12I}{L^3}\right)v_3 = \left(\frac{A}{L} + \frac{12I}{L^3}\right)v_4 \quad (9)$$

In Equation 9, the $\frac{12I}{L}$ term on the left hand side shows that node 2 is stiffer than nodes 3 and 4.

since we define $F_8 = F_{11} = F/2$ and $v_3 = v_4$, Equation 7 and 8 become:

$$F_8 = \frac{F}{2} = \frac{E}{2} \left(\frac{A}{L} + \frac{12I}{L^3} \right) (v_3 - v_2)$$

$$F_{11} = \frac{F}{2} = \frac{E}{2} \left(\frac{A}{L} + \frac{12I}{L^3} \right) (v_4 - v_2)$$

$$F = F_8 + F_{11}$$

define $v_3 = v_4$

$$F = \left(\frac{EA}{L} + \frac{12EI}{L^3} \right) (v_3 - v_2) = \left(\frac{EA}{L} + \frac{12EI}{L^3} \right) (v_4 - v_2) \quad (10)$$

We defined the length of each part of the branch to be equal to half the length of the initial beam we had.

Apply $L = \frac{L_0}{2}$

$$F = \left(\frac{2EA}{L} + \frac{96EI}{L^3} \right) (v_3 - v_2) = \left(\frac{2EA}{L} + \frac{96EI}{L^3} \right) (v_4 - v_2)$$

Take F as $F = \frac{12EI}{L^3}$ as we found for the simple beam example with $v_2 = 1$

For V-type and Y-type branching we can make v_2 fixed so $v_2 = 0$



By taking $v_2 = 0$ and making $v_3 = v_4 = 1$ we find the force required for unit displacement here:

$$F = \left(\frac{2EA}{L} + \frac{96EI}{L^3} \right) v_3 = \left(\frac{8EA}{L} + \frac{96EI}{L^3} \right) v_4$$

if we take $v_3 = v_4 = 1$ we find the Force needed for unit displacement is

$$F = \left(\frac{2EA}{L} + \frac{96EI}{L^3} \right)$$

which is greater than the Force needed for unit displacement of the simple beam, therefore we can say this fractal has a greater stiffness than the simple beam case.

If we define the lengths as in figure 7, then for fixed v_2 equation 10 becomes

$$F = \left(\frac{EA}{\sqrt{1+x^2}} + \frac{12EI}{(1+x)^{\frac{3}{2}}} \right) v_3 = \left(\frac{EA}{\sqrt{1+x^2}} + \frac{12EI}{(1+x)^{\frac{3}{2}}} \right) v_4$$

as x tends to ∞ , F tends to 0 here which would then mean that the stiffness tends to zero also. So maximum stiffness here occurs for x tending towards 0. This means that the T-type branching provides optimum stiffness for v_2 small or equal to zero.

4 Conclusions and Perspectives

While investigating the 3 different types of branching conditions that we looked at for our branching structure, at we discovered that the V-type and T-type are undesirable for optimising transport of media in materials and the Y-type of branching structure is ideal. We discovered that changing the ratio of the diameter of the branches after branching has a notable affect on the flow in the system.

We showed that the T-type branching has optimum stiffness so nature creates Y-type designs to optimise stiffness and flow.

We also showed that the branching structures are stiffer than regular beams of the same length and cross section.

Using Murray's Law we found that a ratio between diameters of $\beta = 0.79$ allows for best flow. Below we have a table which lists the diameter ratios found in blood vessels in both humans [6] and rats [7].

Few of these ratios are close to the optimum value of 0.79. We hypothesise that this is because there is a trade-off between stiffness and flow, since increasing diameter causes an increase in axial stiffness ($A \approx \pi \cdot \frac{d^2}{4}$) which could explain why large blood vessels and arteries with high pressure blood flowing through them have low ratios of β to reduce axial stiffness. We saw that the stiffnesses also depend on $\frac{1}{L}$ and $\frac{1}{L^3}$, meaning that an increase in length corresponds to a decrease in flexural stiffness.

It is also possible that our model only considers two branching pipes instead of many since different number of branches has their own optimal diameter ratios. It is not that odd to find that the actual ratios differ from what is expected as our assumption is too simple in the first place.

There are a lot of interesting future prospects which could be researched if this model is developed further. It could be used to compute stiffnesses in different biological materials such as the lungs, blood vessels, xylem



Human	Diameter	Ratio
aorta	10	
large arteries	3	0.3
main branches	1	0.33
secondary branches	0.6	0.6
tertiary branches	0.14	0.23
terminal arteries	0.05	0.357
terminal branches	0.03	0.6
arterioles	0.02	0.67
capillaries	0.008	0.4

Rat	Diameter	Ratio
Artery	52.6	
Small Artery	19	0.36121673
Arteriole	7	0.368421053
Capillary	3.7	0.528571429

Table 1: Diameter of blood vessels from human and rat

tubes in leaves and plants. It would be interesting to see if there is a relation between fractal dimension of the structure and its flow and stiffness. There is opportunity also for this theory to be expanded into engineering design to create structures that maximise flow of media inside them while also providing enough stiffness to be reliable.

There are some considerations our model does not include which could be improved upon, for example, we only consider open systems in our model. We did not consider a closed loop system. We also did not factor in some other reasons why fractals occur in nature such as to utilise as much space as possible for absorption of air or sunshine in the case of the lungs or flowers.

5 Bibliography

References

- [1] Juan Garcia-Ruiz and Fermin Otálora. “Fractal trees and Horton’s laws”. In: *Mathematical Geology* 24 (Mar. 1992), pp. 61–71. DOI: [10.1007/BF00890088](https://doi.org/10.1007/BF00890088).
- [2] Riccardo Rigon et al. “Optimal Channel Networks - a Framework for the Study of River Basin Morphology”. In: *Water Resources Research* 29 (June 1993), pp. 1635–1646. DOI: [10.1029/92WR02985](https://doi.org/10.1029/92WR02985).
- [3] Harsh Sharma. *Basics of finite element method-direct stiffness method part 1*. July 2020. URL: <https://ichbinharsh.medium.com/basics-of-finite-element-method-direct-stiffness-method-part-1-2676f3ee062a>.
- [4] Marcelo Epstein and Samer Adeeb. “The stiffness of self-similar fractals”. In: *International Journal of Solids and Structures - INT J SOLIDS STRUCT* 45 (June 2008), pp. 3238–3254. DOI: [10.1016/j.ijsolstr.2008.01.022](https://doi.org/10.1016/j.ijsolstr.2008.01.022).
- [5] Samer Adeeb and Marcelo Epstein. “Fractal elements”. In: *Journal of Mechanics of Materials and Structures - J MECH MATER STRUCT* 4 (May 2009), pp. 781–797. DOI: [10.2140/jomms.2009.4.781](https://doi.org/10.2140/jomms.2009.4.781).
- [6] John A. Adam. “Blood Vessel Branching: Beyond the Standard Calculus Problem”. In: *Mathematics Magazine* 84.3 (2011), pp. 196–207. DOI: [10.4169/math.mag.84.3.196](https://doi.org/10.4169/math.mag.84.3.196).
- [7] MARY P. WIEDEMAN. “Dimensions of Blood Vessels from Distributing Artery to Collecting Vein”. In: *Circulation Research* 12.4 (1963), pp. 375–378. DOI: [10.1161/01.res.12.4.375](https://doi.org/10.1161/01.res.12.4.375).